INTERNATIONAL JOURNAL OF ROBUST AND NONLINEAR CONTROL
Int. J. Robust. Nonlinear Control 2011; **00**:1–20
Published online in Wiley InterScience (www.interscience.wiley.com). DOI: 10.1002/rnc

Target Tracking of Autonomous Robotic Vehicles using Range-only Measurements: A Switched Logic-Based Control Strategy

Omid Namaki-Shoushtari[1], A. Pedro Aguiar[2*], and Ali Khaki Sedigh[1]

[1]*Faculty of Electrical and Computer Engineering, K.N. Toosi University of Technology, Tehran, Iran*
[2]*Laboratory of Robotics and Systems in Engineering and Science (LARSyS), Instituto Superior Técnico (IST), Technical University of Lisbon, Portugal*

SUMMARY

This paper considers the pursuing or target tracking problem where an autonomous robotic vehicle is required to move towards a maneuvering target using range-only measurements. We propose a switched logic-based control strategy to solve the pursuing problem that can be described as comprising a continuous cycle of two distinct phases: i) the determination of the bearing, and ii) the steering control of the vehicle to follow the direction computed in the previous step while the range is decreasing. We provide guaranteed conditions under which the switched closed-loop system achieves convergence of the relative distance error to a small neighborhood around zero. Simulation results are presented and discussed. Copyright © 2011 John Wiley & Sons, Ltd.

Received . . .

KEY WORDS: Target tracking; Range-only measurements; Switching control; Autonomous robotic vehicles; Averaging theory

1. INTRODUCTION

The problem of tracking a moving target, which can be another robotic vehicle, by an autonomous robotic vehicle has received special attention in the literature. Particular examples can be found in the area of wheeled mobile robots (e.g., [1–3]), aircraft vehicles (e.g., [4–6]), and marine vehicles (e.g. [7–13]).

*Correspondence to: Institute for Systems and Robotics, Instituto Superior Tecnico, Av. Rovisco Pais 1, 1049-001 Lisbon, Portugal. E-mail: pedro@isr.ist.utl.pt

Contract/grant sponsor: This work was supported in part by projects Co3-AUVs (EU FP7 under grant agreement No. 231378), CONAV/FCT-PT(PTDC/EEA-CRO/113820/2009), CMU- Portugal program, and the FCT ISR/IST plurianual funding program.

In spite of the wide range of applications and the large number of control strategies developed, most of them rely on the assumption that both the bearing (line-of-sight angle) and the range (relative distance between the vehicle and the target) are known for navigation, guidance and control purposes.

In this paper, we are interested in the problem when the only information available about the target is the range. This type of problems is motivated by applications in several domains, e.g., wireless networks, surveillance, marine applications, localization [14–17]. In our particular case, the practical motivation arises from applications to autonomous underwater vehicles (AUVs), where the range is obtained by measuring the time-of-flight of an acoustic pulse. An interesting and attractive scenario is the case when a surface craft is performing a maneuver along a predefined path, while an AUV in a configuration master/slave is required to follow the surface craft. Note that the surface craft can use GPS for localization, but the AUV cannot because electromagnetic waves do not propagate well underwater. To overcome this problem, an alternative but challenging solution (compared with the costly traditional methods) is to make both the vehicles to carry on-board an acoustic modem and with this setup being able to compute the range between them. From a theoretical point of view the control problem is challenging because the overall system is nonlinear and there exist conditions that make the system unobservable. One well known example is when both the target and the pursuer vehicles are moving in a straight line. In this case, it can be seen that there exist several initial conditions that lead to the same output signal (in this case the same range).

The target tracking problem using range-only measurements has been recently addressed in [18], where the authors propose a sliding mode control law to steer a Dubins-like wheeled robot towards a target that moves with a constant speed while preserving a predefined range margin from the target. The proposed strategy ultimately makes the robot to move around the target along a circular trajectory. The radius of circle or the preserved margin from the target is predefined with a control parameter. Equiangular Navigation Guidance algorithms for approaching and following both steady and moving targets with range-only measurements are proposed in [19]. With constant robot linear velocity, the robot-target range variation is used as a measure for the angle at which the robot approaches the target. The proposed guidance methods have the property that the trajectory of the controlled robot is close to a certain curve called an equiangular spiral. A different strategy is described in [20–22] where the problem of seeking the source of a scalar signal (stationary target) using a non-holonomic vehicle with no position information was solved using an extremum seeking approach.

It is important to stress that the few solutions described in the literature are in many cases not suitable for the surface-craft/AUV application scenario because the resulting trajectories are “not natural” in the sense that it would make the AUV to deviate too much from the surface craft.

This paper addresses the pursuing or target tracking problem in 2D, where an autonomous robotic vehicle is required to move towards a steady or maneuvering target. The robotic vehicle does not have the capability of sensing its position or the position of the target. The only available information

DOI: 10.1002/rnc

about the target is the range (relative distance) between the pursuer and the target. We propose a novel switched logic-based control strategy that can be described as comprising a continuous cycle of two distinct phases: i) the determination of the bearing, and ii) the steering control of the pursuer to follow the direction computed in the previous step while the range is decreasing. In the first phase, inspired by the extremum seeking approach, the control strategy is to keep the forward velocity constant and actuate on the angular velocity so that the vehicle will move in a "persistence of excitation" mode to obtain the bearing of the target. The bearing is obtained by averaging the measurements of vehicle heading. In the second phase, the main idea is to actuate on the linear and angular velocities so that the vehicle will follow the direction of the bearing computed in the first phase and converge to a neighborhood of the target. A supervisor switching control law coordinates which phase and when, of these two modes are enabled. Resorting to Lyapunov and averaging theory, the stability of the overall switched system is analyzed and conditions for the convergence of the relative distance error are derived. The key novel contribution of this work with respect to the references above is the fact that the proposed control strategy guarantees convergence of the relative distance error for moving targets and the resulting trajectories are more suitable to be applied in the AUV scenario. To illustrate the effectiveness and performance of the proposed control scheme, we present simulation results for the following three scenarios: the target is stationary, the target moves in a straight line and the target performs a lawn mowing maneuver.

This paper is organized as follows: Section 2 formulates the target tracking problem and describes the vehicle model. Section 3 presents the switched control algorithm and in Section 4, the stability of the overall closed-loop system is analyzed. Simulation results and conclusions are included in Sections 5 and 6, respectively.

2. PROBLEM FORMULATION

Consider an autonomous robotic vehicle moving in horizontal plane (see Figure 1) and let $(x, y, \theta) \in SE(2)$ denote the configuration of an inertial coordinate frame $\{B\}$ with respect to a body-fixed frame $\{U\}$ that satisfies

$$\dot{x} = u_1 \cos\theta, \tag{1a}$$

$$\dot{y} = u_1 \sin\theta, \tag{1b}$$

$$\dot{\theta} = u_2, \tag{1c}$$

where $(x, y)^T$ is the position of the center of mass of the vehicle, θ its orientation, and u_1 and u_2 are the body-fixed linear and angular velocities, respectively. Consider also a second vehicle (the target

Prepared using rncauth.cls
DOI: 10.1002/rnc

vehicle) with the following associated equations of motion

$$\dot{x}_t = V_t \cos\theta_t, \tag{2a}$$

$$\dot{y}_t = V_t \sin\theta_t, \tag{2b}$$

$$\dot{\theta}_t = \omega_t, \tag{2c}$$

where the position and orientation $(x_t, y_t, \theta_t) \in SE(2)$, which are defined with respect to $\{U\}$, and the velocities V_t and ω_t are all *unknown signals* to the first vehicle.

Suppose that the first vehicle is equipped with a set of sensors that provide the measurement of the angle θ and the distance (range) from the sensor position located at R away from the center of mass

$$\begin{pmatrix} x_s \\ y_s \end{pmatrix} = \begin{pmatrix} x \\ y \end{pmatrix} + R \begin{pmatrix} \cos\theta \\ \sin\theta \end{pmatrix}, \tag{3}$$

to the position of the target vehicle, that is, $r := \sqrt{(x_t - x_s)^2 + (y_t - y_s)^2}$. See Figure 1.

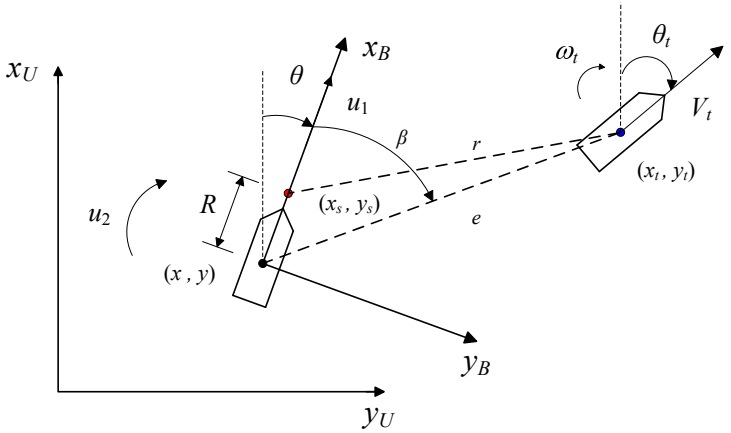

Figure 1. Setup for the pursuing control problem.

The control problem considered in this paper can be formulated as follows:
Using as only measurements the orientation θ and the range r, derive a feedback law for $u = (u_1, u_2)$ such that for every initial condition in a predefined set $J \subset SE(2)$ the vehicle's center of mass (x, y) converges to a predefined ball $B_\epsilon(x_t, y_t)$ with center (x_t, y_t) and radius $\epsilon > 0$.

3. SWITCHED LOGIC-BASED CONTROL DESIGN

This section presents a control strategy to solve the challenging pursuing problem stated above. The proposed solution can be described as comprising a continuous cycle of two distinct phases:
Phase 1: The determination of the bearing, so that the vehicle will be able to point to the target. Note that in this stage, the vehicle will have to move in a "persistence of excitation" mode.

Prepared using rncauth.cls
DOI: 10.1002/rnc

Phase 2: The steering control of the vehicle to follow the direction computed in the previous step while the (estimated) rate of change of the range r is greater than some acceptable value. Switch to step (1) when this does not hold.

3.1. Phase 1: The determination of the bearing

In this stage the goal is to compute, using as measurements the range r and the heading θ, the (correct) bearing so that the vehicle will be able to point to the target. To accomplish this task, we propose a feedback law that acts on the angular velocity u_2 and keeps the forward velocity u_1 constant. To this effect, inspired by the extremum seeking approach, we propose the control law

$$u_1 = V_c, \tag{4a}$$

$$u_2 = k_1 \omega \cos(\omega t) + k_2 \xi \sin(\omega t), \tag{4b}$$

where ξ is the output of the following system

$$\dot{\chi} = -\lambda\,(\chi + r^2), \tag{5a}$$

$$\xi = -(\chi + r^2), \tag{5b}$$

and $k_1,\ k_2$, $\lambda,\ V_c$, and ω are positive control parameters. To compute the bearing at time $t = T$, we propose to average $\theta(t)$, that is,

$$\bar{\theta} = \frac{1}{T}\int_0^T \theta(s)\, ds. \tag{6}$$

Note that in (4b) we are forcing the angular velocity of the vehicle to have an oscillation of frequency ω. This excitation signal will consequently lead to an oscillation on the vehicle's heading. In Section 4 we show that after a few oscillations, the average heading can be used as a desired orientation to steer the vehicle towards the target.

3.2. Phase 2: Following a constant direction

In this phase, we propose the feedback law

$$u_1 = k_3\, r \tag{7a}$$

$$u_2 = -k_4(\theta - \bar{\theta}), \tag{7b}$$

where $\bar{\theta}$ is the desired direction computed at the end of phase 1 and $k_3,\ k_4$ are positive gains to be chosen properly. Notice that, since $\bar{\theta}$ is constant in this stage, the vehicle will follow "blindly" the target. It may be possible that during this stage the target may change its direction so that $\bar{\theta}$ may not be a good measure of the bearing. To detect this situation, we estimate the rate of change of r and compare it with a given threshold that depends on the linear velocity u_1. To estimate $\dot{r}$, we propose

DOI: 10.1002/rnc

a Kalman filter designed according to the linear model

$$\dot{r} = V_r + w_1, \tag{8a}$$

$$\dot{V}_r = w_2, \tag{8b}$$

$$y = r + v \tag{8c}$$

where (r, V_r) is the state, y is the measured output, and $w = (w_1, w_2)$ and v are assumed to be mutually independent stationary, Gaussian, zero mean white noise processes.

Remark 1: For simplicity, the feedback law (7) was derived without taking into account the problem of input saturation. However, in Appendix we show that the saturated feedback laws

$$\begin{aligned} u_1 &= k_3^a \tanh(k_3^b\, r) \\ u_2 &= -k_4^a \tanh\left(k_4^b\,(\theta - \bar{\theta})\right) \end{aligned} \tag{9}$$

instead of (7) would also work by selecting the proper values for the gains $k_i^a, k_i^b > 0$, $i = 3, 4$.

□

3.3. *Switched Controller*

Let $\sigma : [t_0, \infty) \to \{1, 2\}$ be a piecewise constant switching signal that is continuous from the right and evolves according to

$$\sigma(t) = \begin{cases} 1\,, & t \in [t_{i-1}\,, t_i)\,,\ i \ \text{ odd}\,, i \in \mathbb{N} \\ 2\,, & t \in [t_{i-1}\,, t_i)\,,\ i \ \text{ even}, i \in \mathbb{N} \end{cases} \tag{10}$$

In (10), $\{t_0, t_1, t_2, t_3, ...\}$ is a sequence of strictly increasing infinite switching times in $[t_0, \infty)$ and $t_0 = 0$ is the initial time. The switching controller is given by

$$u = \alpha_\sigma(\theta, r),$$

where $\alpha_1(\cdot)$ corresponds to the control law (4)-(5) and $\alpha_2(\cdot)$ to the control law (7). In (10), when i is odd (σ =1) we set

$$t_i = t_{i-1} + nT\,,\ T = \frac{2\pi}{\omega}$$

for some given $n \in \mathbb{N}$. For i even (σ =2) we set t_i as the time t such that

$$t_i = \max\left\{ t_{i-1} + \Delta,\ \min_t \{t \geq t_{i-1} : \hat{V}_r(t) \geq -\delta\,\} \right\} \tag{11}$$

where $\delta > 0$ is a given threshold, $\hat{V}_r$ is the estimate of $\dot{r}$ using the Kalman filter described in Section 3.2, and $\Delta > 0$ is a dwell time ([23] and [24]) to enforce that the second controller will be enabled at least Δ seconds. It is important to stress that the only input signals of the overall control law (as it

Prepared using rncauth.cls
DOI: 10.1002/rnc

can be seen from (4-5) and (7)) are only the range r and the heading of the vehicle θ. The controller does not need the rate of r neither the bearing angle.

4. STABILITY ANALYSIS

In this section, we analyze the stability of the closed-loop system. To this effect, we first introduce the following variables. Let e (see Figure 1) denote the position error between (x, y) and (x_t, y_t), that is,

$$e = \sqrt{(x - x_t)^2 + (y - y_t)^2}, \tag{12}$$

and β the angle between the vector x_B and the vector defined by (x, y) and (x_t, y_t). From Figure 1, it follows that

$$x - x_t = -e\,\cos(\theta + \beta), \tag{13a}$$

$$y - y_t = -e\,\sin(\theta + \beta), \tag{13b}$$

where $\theta + \beta = \tan^{-1}\left(\frac{-(y-y_t)}{-(x-x_t)}\right)$. Using the above equations, one can compute (see Appendix) the dynamics for e and β to arrive to

$$\dot{e} = -u_1 \cos\beta + V_t \cos(\beta + \theta - \theta_t), \tag{14}$$

$$\dot{\beta} = \frac{u_1}{e}\sin\beta - u_2 - \frac{V_t}{e}\sin(\beta + \theta - \theta_t). \tag{15}$$

We now provide conditions for the convergence of $\bar{\theta}$ defined in (6) to the correct bearing $\bar{\theta}^\star$, which satisfies (see Figure 1)

$$\bar{\theta}^\star = \theta + \beta.$$

Theorem 1

Let Σ_1 denote the closed-loop system that results from the feedback interconnection of (1) with (4). Let $e^\star > 0$ and $\epsilon > 0$ be given allowable tolerant position and orientation errors, respectively, and $D_{[0,t_f]}$ the largest set in $\mathbb{R}^3$ such that for every initial condition $(x, y, \theta)(0) \in D_{[0,t_f]}$, the solution of Σ_1 is well defined for all $t \in [0, t_f]$ with $e(t) \geq e^\star$. Let $k_2 > 0$ be a sufficiently large gain such that the following holds

$$V_c \leq 2\,\frac{J_1(k_1)}{J_0(k_1)}\,k_2\,R\,e^\star - \frac{\gamma}{J_0(k_1)} \tag{16}$$

with $V_c > 0$ and $\gamma > V_t$. In (16), $J_0(k_1)$ and $J_1(k_1)$ denote the Bessel integral equalities (Bessel functions of the first kind, see e.g., [25]) given by

$$\begin{aligned} J_0(k_1) &= \frac{1}{2\pi}\int_0^{2\pi} e^{jk_1\,\sin(t)}\,dt \\ J_1(k_1) &= \frac{-j}{2\pi}\int_0^{2\pi} e^{jk_1\,\sin(t)}\sin(t)\,dt \end{aligned}$$

Prepared using rncauth.cls
DOI: 10.1002/rnc

and $k_1 > 0$ is selected such that $J_0(k_1)$ and $J_1(k_1)$ are positive.

Then, there exist a sufficiently large $\omega > 0$ and a positive natural number n such that for every initial condition in $D_{[0,t_f]}$ with $t_f = nT = n\frac{2\pi}{\omega}$,

$$|\bar{\theta}(t_f) - \bar{\theta}^\star(t_f)| \leq \epsilon. \tag{17}$$

Proof

To prove (17) we will show that $\beta = \bar{\theta}^\star - \theta$ converges in average to a small neighborhood around zero. From (15) and using (4), we obtain

$$\dot{\beta} = \frac{V_c}{e}\,\sin\beta\, - k_1\,\omega\cos(\omega t)\, - k_2\xi\sin(\omega t) - \frac{V_t}{e}\,\sin(\beta+\theta-\theta_t).$$

Introducing the following variables

$$\tau \coloneqq \omega t, \tag{18}$$

$$\hat{\beta} \coloneqq \beta + k_1\sin(\tau), \tag{19}$$

$$\hat{\theta} \coloneqq \theta - k_1\sin(\tau), \tag{20}$$

$$\hat{e} \coloneqq \frac{e}{e^\star}, \tag{21}$$

and changing the time scale, it follows that

$$\frac{d\hat{\beta}}{d\tau} = \frac{1}{\omega e^\star}\Big[\frac{V_c}{\hat{e}}\,\sin(\hat{\beta}-k_1\sin\tau)\, - k_2 e^\star\xi\sin(\tau) - \frac{V_t}{\hat{e}}\,\sin(\hat{\beta}+\hat{\theta}-\theta_t)\Big]. \tag{22}$$

We now resort to averaging theory. Since the right-hand side of (22) is periodic in τ with period 2π, applying the average operator $\frac{1}{T}\int_0^T(\cdot)\,d\tau$, one obtains the averaged system

$$\frac{d\hat{\beta}^{avg}}{d\tau} = \frac{1}{\omega e^\star}\Big[\frac{V_c J_0(k_1)}{\hat{e}^{avg}} - 2Rk_2e^\star\hat{e}^{avg}J_1(k_1)\Big]\sin(\hat{\beta}^{avg}) - \frac{V_t}{\omega e^\star}\,\frac{\sin(\hat{\beta}^{avg}+\hat{\theta}^{avg}-\theta_t^{avg})}{\hat{e}^{avg}}.$$

Resorting to Proposition 1 in Appendix with $a_1(t) = -\frac{1}{\omega e^\star}\Big[\frac{V_c J_0(k_1)}{\hat{e}^{avg}} - 2Rk_2e^\star\hat{e}^{avg}J_1(k_1)\Big]$ and $a_2(t) = -\frac{V_t}{\omega e^\star}\,\frac{\sin(\hat{\beta}^{avg}+\hat{\theta}^{avg}-\theta_t^{avg})}{\hat{e}^{avg}}$ and using (16) and the fact that $\hat{e} > 1$, we can conclude that if the initial condition $\hat{\beta}_0^{avg}$ satisfies $|\hat{\beta}_0^{avg}| \leq \cos^{-1}(a) \pmod{2\pi}$, with $a = \sqrt{\frac{\gamma - V_t}{\gamma}}$, then $\hat{\beta}^{avg}$ converges to a neighborhood around zero $(\mathrm{mod}\ 2\pi)$ and satisfies

$$\lim_{t\to\infty}\sup|\hat{\beta}^{avg}(t)| \leq \cos^{-1}(a) \quad (\ \mathrm{mod}\ 2\pi).$$

Using the results in [26] and noticing that the averaged system is a strong average system (see Definition 2 in [26]) we can conclude that for sufficiently large ω, $\hat{\beta}(\tau)$ satisfies

$$\hat{\beta}(\tau) - \hat{\beta}^{avg}(\tau) = O\Big(\frac{1}{\omega e^\star}\Big), \quad \forall\tau \geq 0 \tag{23}$$

Prepared using rncauth.cls
DOI: 10.1002/rnc

From (23) and the fact that $\bar{\theta} = \frac{1}{T}\int_0^T (\bar{\theta}^\star - \beta(\tau))\, d\tau = \bar{\theta}^\star - \frac{1}{T}\int_0^T \hat{\beta}(\tau)\, d\tau$, the result follows. □

Remark 2: Note that in this phase, the distance error between (x, y) and (x_t, y_t) satisfies the dynamics

$$\dot{e} = -V_c \cos\beta + V_t \cos(\beta + \theta - \theta_t).$$

Using (18)-(21), it follows that

$$\frac{d\hat{e}}{d\tau} = \frac{1}{\omega e^\star}\left\{-V_c \cos(\hat{\beta} - k_1 \sin\tau) + V_t \cos(\hat{\beta} + \hat{\theta} - \theta_t)\right\}.$$

By resorting to the method of averaging, we can conclude that the averaged error satisfies

$$\frac{d\hat{e}^{avg}}{d\tau} = \frac{1}{\omega e^\star}\Big[- V_c J_0(k_1) \cos(\hat{\beta}^{avg}) + V_t \cos(\hat{\beta}^{avg} + \hat{\theta}^{avg} - \theta_t^{avg})\Big]. \tag{24}$$

Therefore, in a finite period of time (nT seconds), $\hat{e}^{avg}$ and consequently e is bounded because the right hand-side of (24) is bounded. Furthermore, since $\hat{\beta}^{avg}$ converges to a neighborhood around zero, it can be seen that $\hat{e}^{avg}$ will also decrease its value when $V_c > V_t/(J_0(k_1)\cos(\hat{\beta}^{avg}))$.

□

Next, we examine the stability of the closed loop system when the second stage (following a constant direction) is enable.

Theorem 2

Let Σ_2 denote the closed-loop system that results from the interconnection of (1), (3) with the control law (7). Let $e^\star > R$ be a given allowable tolerant position error, and $D_{[0,t_f]}$ the largest set in $\mathbb{R}^3$ such that for every initial condition $(x, y, \theta)(0) \in D$, the solution of Σ_2 is well defined for all $t \in [0, t_f]$ with $e(t) \geq e^\star$ and the error between the real bearing $\bar{\theta}^\star$ and $\bar{\theta}$ defined as $\tilde{\bar{\theta}} = \bar{\theta}^\star - \bar{\theta}$ remains bounded by some $\epsilon > 0$, that is, $\sup_{0\leq t\leq t_f} |\tilde{\bar{\theta}}| \leq \epsilon$. Let k_4 be a positive gain such that the following holds:

$$2\,\frac{k_3}{k_4} + \epsilon + \frac{V_t}{e^\star\, k_4} < \frac{\pi}{2}. \tag{25}$$

Then, for sufficiently large gain k_3 the position error e converges to a neighborhood around zero with ultimate bound less or equal than $e^\star$.

Proof

The proof is organized as follows. First, it will be shown that β is ultimately bounded with the ultimate bound less than $\frac{\pi}{2}$. Using this fact, we then prove the convergence of e. Consider the dynamics of β (see (15)), which in closed-loop satisfies

$$\dot{\beta} = \frac{k_3\, r}{e}\sin\beta + k_4(\theta - \bar{\theta}) - \frac{V_t}{e}\sin(\beta + \theta - \theta_t). \tag{26}$$

From Figure 1 it follows that

$$r^2 = e^2 + R^2 - 2Re\cos\beta,$$

Prepared using rncauth.cls
DOI: 10.1002/rnc

which implies that r can be written in the form

$$r = e + f(e, R, \beta), \tag{27}$$

where $f(e, R, \beta)$ is a bounded function with $|f| \leq R$. Now, consider the positive definite function $V_1(\beta) \coloneqq \frac{1}{2}\beta^2$. Computing its time derivative along the trajectories of (26), using (27) and the fact that $\theta - \bar{\theta} = -(\beta - \tilde{\bar{\theta}})$, one obtains

$$\begin{aligned}
\dot{V}_1 &= \beta\left[k_3 \frac{e+f}{e}\sin\beta - k_4(\beta - \tilde{\bar{\theta}}) - \frac{V_t}{e}\sin(\beta + \theta - \theta_t)\right] \\
&\leq -k_4\beta^2 + |\beta|\,[2k_3 + k_4\,\epsilon + V_t/e^\star] \\
&= -k_4(1-\alpha)\beta^2 - \alpha k_4\beta^2 + |\beta|\,[2k_3 + k_4\,\epsilon + V_t/e^\star]\,, \\
&\leq -k_4(1-\alpha)\beta^2, \quad \forall\,|\beta| \geq \frac{2k_3 + k_4\,\epsilon + V_t/e^\star}{k_4\alpha}
\end{aligned}$$

where α is any scalar that satisfies $0 \leq \alpha < 1$. From this it follows that if the gain k_4 is selected as in (25), β will be ultimately bounded with the ultimate bound β_a less than $\frac{\pi}{2}$.

We are now ready to prove the convergence of e. From (14), with $u_1 = k_3\, r$, see (7a), and using (27) the dynamics of e satisfies

$$\dot{e} = -k_3\,(e + f)\cos\beta + V_t\cos(\beta + \theta - \theta_t).$$

Let $V_2(e) \coloneqq \frac{1}{2}e^2$. Its time-derivative satisfies

$$\begin{aligned}
\dot{V}_2 &\leq -k_3 e^2\cos\beta + |e|\,(V_t + k_3 R), \\
&= -k_3(1-\alpha)e^2\cos\beta - \alpha k_3 e^2\cos\beta + |e|\,(V_t + k_3 R), \\
&\leq -k_3(1-\alpha)e^2\cos\beta,\ \forall\,|e| \geq \frac{V_t}{k_3\alpha\cos\beta} + \frac{R}{\alpha\cos\beta}
\end{aligned} \tag{28}$$

for $0 \leq \alpha < 1$. From (28) we can conclude that for any finite time $t \geq 0$, $e(t)$ is bounded (that is, there is no finite escape) and furthermore, after a finite time t_1 with $|\beta(t_1)| < \frac{\pi}{2}$, $e(t)$ will converge to a neighborhood around zero of size less than $e^\star$, provided that k_3 is sufficiently large and $e^\star > R/\cos(\beta_a)$. □

We can now conclude that according to the switching rule described in Section 3.3 and resorting to Theorem 1 and 2, if the switching between these two phases is slowed down by a sufficiently large dwell time τ_D such that $\min(nT, \Delta) \geq \tau_D$, based on the results in ([23] and [24]) the switched closed-loop system is bounded (that is all the states are bounded) and there exists an $\epsilon > 0$ such that while $e(t) > \epsilon$ the vehicle will converge towards the target and will remain afterwards around the target. This behavior will be illustrated in the next section.

Prepared using rncauth.cls
DOI: 10.1002/rnc

5. SIMULATION RESULTS

This section illustrates the performance of the proposed control scheme through computer simulations. We present three scenarios: *i)* stationary target, *ii)* the target moves along a straight line, and *iii)* the target performs a lawn mowing maneuver. The initial configurations of the pursuer and the target vehicles are respectively $(x, y, \theta)(0) = (0, 0, 0)$ and $(x_t, y_t, \theta_t)(0) = (50m, 50m, 0)$. The target linear velocity was set to $V_t = 0.2m/s$. The control parameters were selected as follows: $\omega = 0.5rad/sec$, $R = 0.5m$, $k_1 = 1$, $k_2 = 1$, $k_3^a = 1.6$, $k_3^b = 0.02$, $k_4 = 10$, $\lambda = 1$, $e^\star = 1m$, and $V_c = 0.2m/s$. The criteria used to select them was based on the following procedure: *i)* for phase 1 (extremum seeking control based algorithm), k_1 and ω are the amplitude and frequency of the probing signal that is injected to the system to get a measure of the gradient information of $-r^2$. It was noted that the vehicle will make sharper turns as the parameter k_1 is increased. The parameter ω should be also sufficiently large as it is required in Theorem 1. The signal $-r^2$ is filtered by a high pass filter of the form $\frac{s}{s+\lambda}$ to remove the DC (and low frequency) components, where λ is the cut-off frequency of the filter. The parameter k_2 can be seen as an adaptation gain and should satisfy (together with k_1) the conditions of Theorem 1; *ii)* In phase 2, k_3^a, k_3^b, and k_4 are used to tune the convergence behavior of e and $\theta - \bar{\theta}$ to zero. In the simulation, we consider the realistic case that the vehicle has dynamics (to capture the effect that the velocities cannot change instantaneously) and input saturations. To take into account those effects we include a first-order filter with input saturation that emulates the dynamics of the vehicle in closed-loop with an inner-loop controller that is responsible to drive the actual velocity of the vehicle to the desired one.

5.1. *Stationary target*

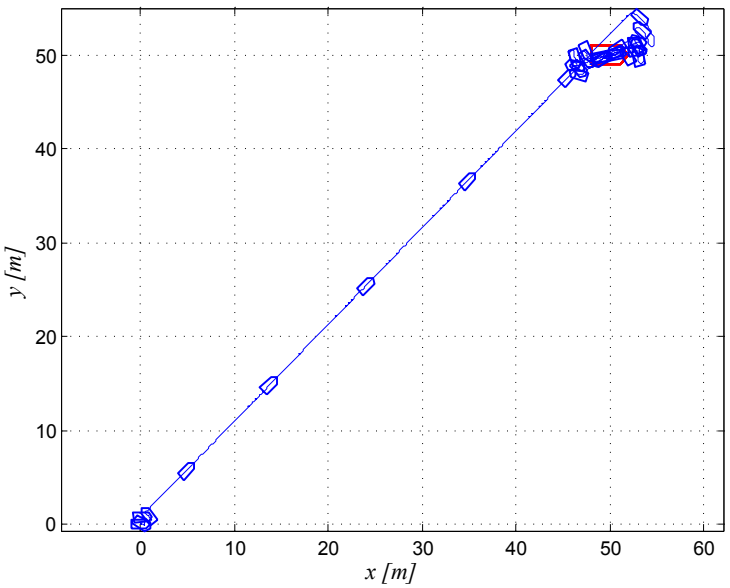

Figure 2. Simulation path of the pursuer vehicle (stationary target).

DOI: 10.1002/rnc

Figure 2 illustrates the path of the vehicle for a stationary target. It can be seen that the vehicle converges to and stay in a neighborhood of the target. This is corroborated in Figure 4, where both the components of the position error e converge to a neighborhood of zero. Figure 3 shows the time evolution of the forward velocity and the control input u_1.

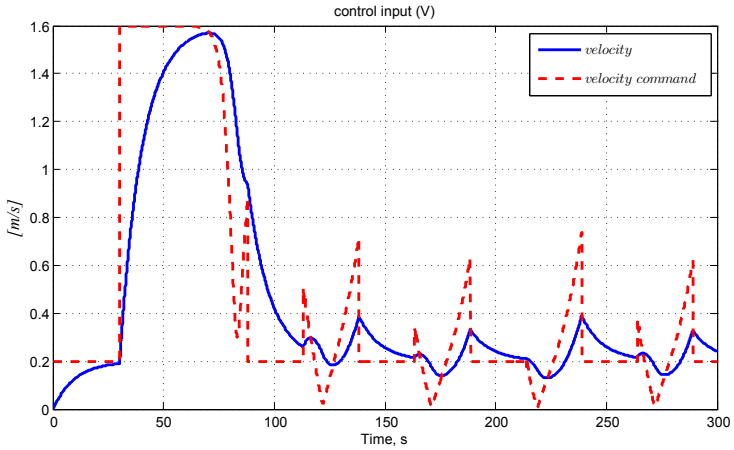

Figure 3. Time evolution of the forward velocity and the velocity command of the pursuer vehicle for the stationary target case.

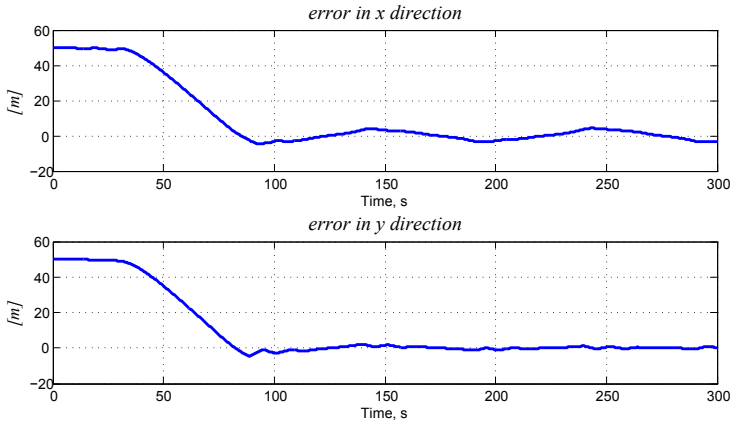

Figure 4. Time evolution of the components of the error vector $(x - x_t, y - y_t)$ for the stationary target case.

5.2. *The target moves along a straight line*

In this scenario the target vehicle moves along a straight line with $V_t = 0.2\,m/s$. Figure 5 displays the resulting trajectories of the vehicles where it can be seen that the pursuer moves towards the target. Notice also that the pursuer vehicle is constantly switching between the two modes. This behavior is clearly seen in Figure 6 that shows the "steady-state" trajectories of the last 40 meters of the vehicles in the simulation. It is important to point out that the pursuer cannot perform for all time a straight-line motion because in this mode the system is not observable.

Prepared using rncauth.cls
DOI: 10.1002/rnc

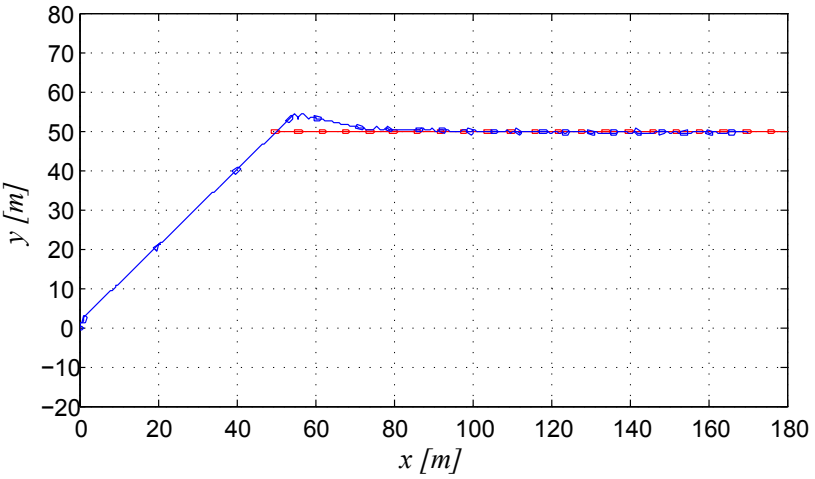

Figure 5. Simulation paths of the pursuer and the target vehicles for the case that the target vehicle moves on a straight line.

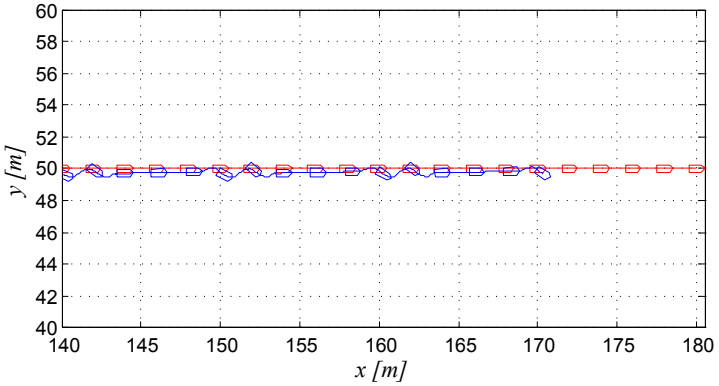

Figure 6. Zoom in of the last 40 meters of the pursuer and target vehicles maneuvers shown in Figure 5 (steady-state trajectories).

5.3. The target performs a lawn mowing maneuver

Figures 9-11 show the simulation results when the pursuer vehicle is required to track a target vehicle that is performing a lawn mowing maneuver composed by straight lines and arcs. From the figures, it can be seen that the vehicle is capable to converge to the target and follow it. However, as it is expected, the distance error increases when the target is on the arc phase. In this simulation, in the last straight line (after the curve) the target velocity V_t is changed abruptly from 0.2 to 0.1 m/s. In order to attenuate the oscillation in speed of the vehicle when the proposed strategy switches again to phase 1, V_c was set to be $u_1(t_i^-)$, where $u_1(t_i^-)$ denote the velocity of the vehicle before switch to phase 1. Note that the pursuer vehicle still has a good tracking performance even without knowing that the target has changed its speed.

Prepared using rncauth.cls
DOI: 10.1002/rnc

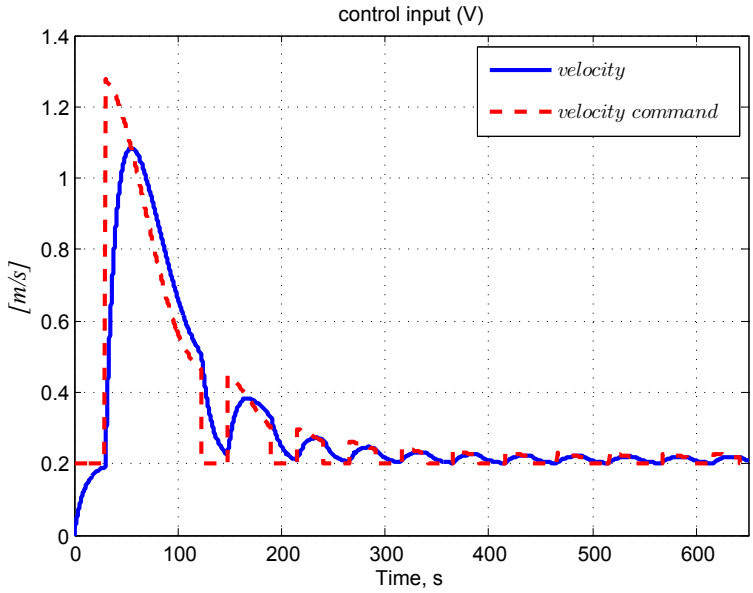

Figure 7. Time evolution of the forward velocity and the velocity command of the pursuer vehicle for the case that the target vehicle moves on a straight line.

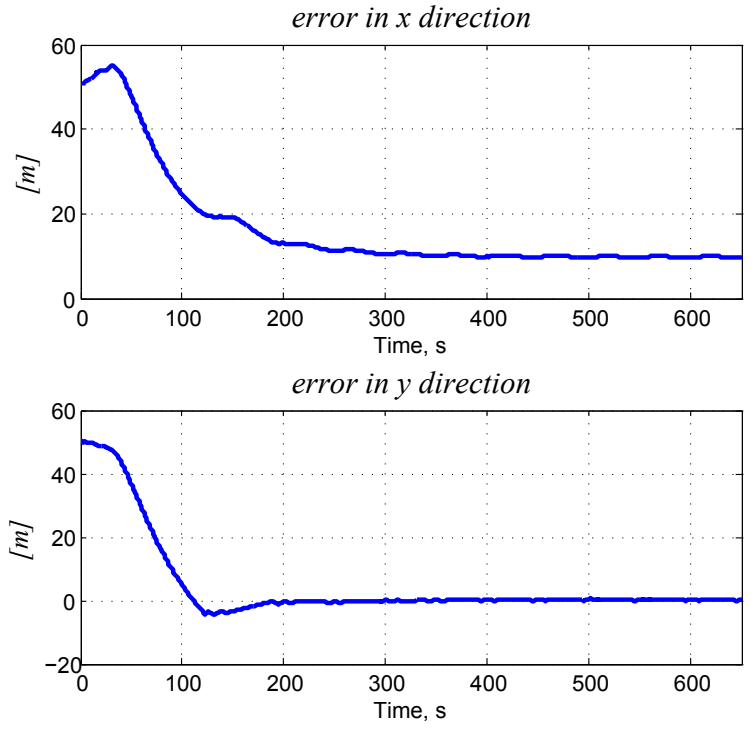

Figure 8. Time evolution of the components of the error vector $(x - x_t, y - y_t)$ for the case that the target vehicle moves on a straight line.

DOI: 10.1002/rnc

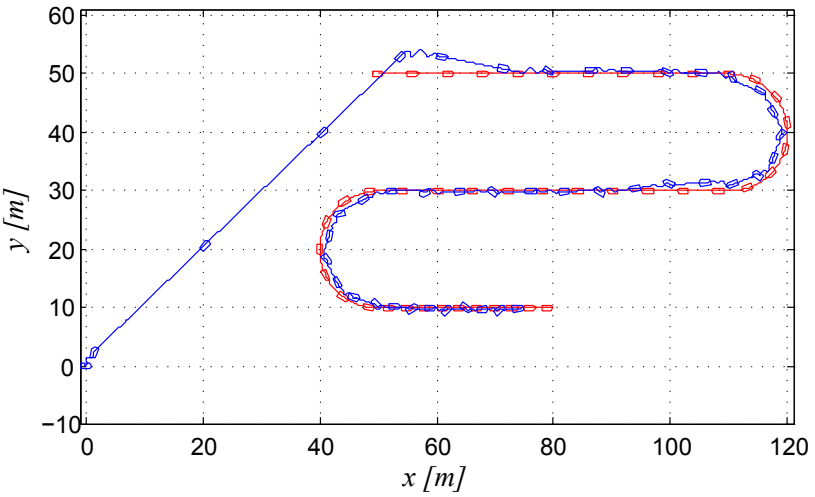

Figure 9. Simulation paths of the pursuer and the target vehicles for the case that the target is performing a lawn mowing maneuver.

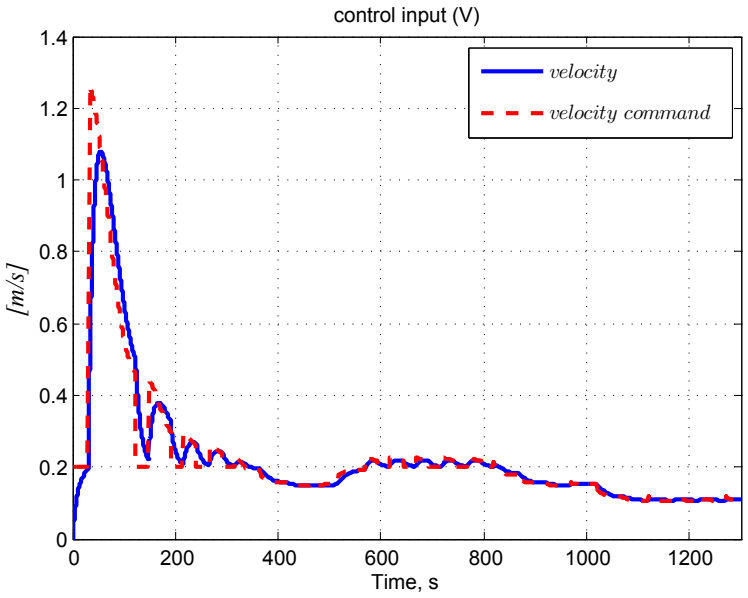

Figure 10. Time evolution of the forward velocity and the velocity command of the pursuer vehicle for the case that the target is performing a lawn mowing maneuver.

6. CONCLUSION

In this paper, we addressed the target tracking problem where an autonomous robotic vehicle is required to move towards a maneuvering target using range-only measurements. We proposed a switched based control strategy to solve the pursuing problem that unfolds in two distinct phases: i) the determination of the bearing, and ii) following the direction computed in the previous step, while the range is decreasing. We provided guaranteed conditions under which the switched closed-loop system achieves convergence of the relative distance error to a small neighborhood around zero.

Prepared using rncauth.cls
DOI: 10.1002/rnc

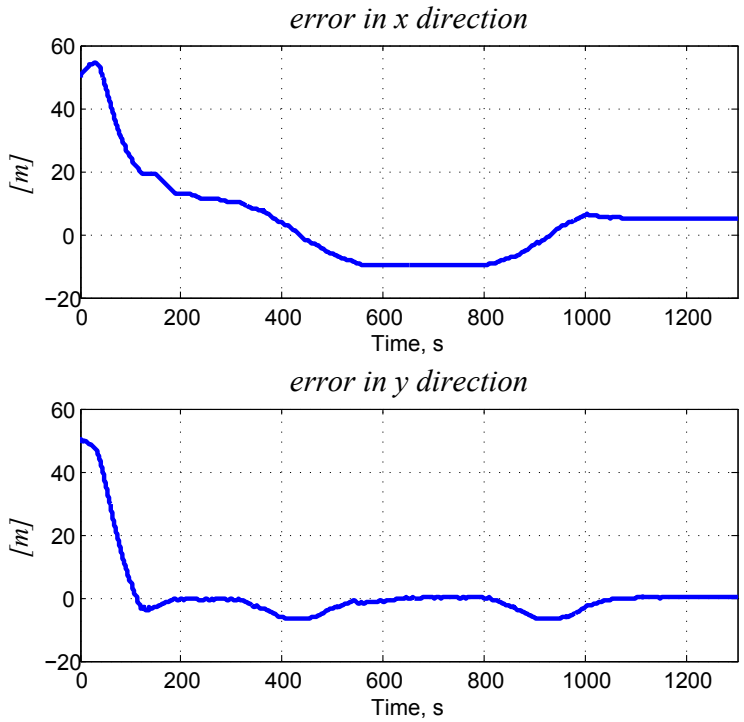

Figure 11. Time evolution of the components of the error vector $(x - x_t, y - y_t)$ for the case that the target is performing a lawn mowing maneuver.

The simulation results showed the good performance of the proposed solution. An issue for future research is the integration of an obstacle avoidance system in the proposed tracking algorithm. A promising strategy is to follow some of the ideas in [19].

APPENDIX

Proposition 1

Consider the following scalar system

$$\dot{\beta} = -a_1(t)\sin(\beta) + a_2(t), \quad \beta(0) = \beta_0 \tag{29}$$

where $a_1(t)$ and $a_2(t)$ are assumed to be bounded piecewise continuous signals with $a_1(t) \geq \underline{a}_1$, $|a_2(t)| \leq \bar{a}_2, \forall t \geq 0$, and $\underline{a}_1 > \bar{a}_2 > 0$. Then for every initial condition

$$|\beta_0| \leq \cos^{-1}(a),\ a = \sqrt{\frac{\underline{a}_1 - \bar{a}_2}{\underline{a}_1}}, \quad (\mod 2\pi)$$

$\beta(t)$ converges to a neighborhood around zero ($\mod 2\pi$) and satisfies

$$\lim_{t\to\infty} \sup |\beta(t)| \leq \cos^{-1}(a) \quad (\mod 2\pi). \tag{30}$$

Prepared using rncauth.cls
DOI: 10.1002/rnc

In particular, if $a_2(t)$ is identically zero, then for almost every initial condition, $\beta(t)$ converges to zero ($\mathrm{mod}\ 2\pi$).

Proof

Consider the Lyapunov function candidate

$$V = 1 - \cos\beta$$

whose time derivative along (29) satisfies

$$\begin{aligned}\dot{V} &= -a_1(t)\sin^2\beta + a_2(t)\sin\beta \\ &= -a_1(t)(1+\cos\beta)(1-\cos\beta) + a_2(t)\sin\beta \\ &\leq -\underline{a}_1(2-V)V + \bar{a}_2\end{aligned}$$

Thus, by noticing that $0 \leq a < 1$ it can be verified that if $V_0 < 1 + a$, then $\lim_{t\to\infty} \sup V(t) \leq 1 - a$, which implies (30). □

Derivation of equations (14) and (15)

According to Figure 1 the position error between (x, y) and (x_t, y_t) is given by (12) and the angle $\beta + \theta$ satisfies (13). Using (1), (2) and (13), the time derivative of e can be obtained as follows:

$$\begin{aligned}\dot{e} &= \left[(\dot{x} - \dot{x_t})(x - x_t) + (\dot{y} - \dot{y_t})(y - y_t)\right]/e \\ &= -\cos(\theta+\beta)\left(u_1\cos\theta - V_t\cos\theta_t\right) - \sin(\theta+\beta)\left(u_1\sin\theta - V_t\sin\theta_t\right),\end{aligned}$$

which yields (14) by resorting to simple trigonometric equalities. To obtain (15) note that $\theta + \beta = \tan^{-1}\left(\frac{-(y-y_t)}{-(x-x_t)}\right)$. Taking its time-derivative yields

$$\dot{\theta} + \dot{\beta} = \frac{\frac{(\dot{y}-\dot{y_t})(x-x_t) - (\dot{x}-\dot{x_t})(y-y_t)}{(x-x_t)^2}}{1 + \frac{(y-y_t)^2}{(x-x_t)^2}}$$

Using (1), (2), and (13) it follows that

$$\dot{\theta} + \dot{\beta} = \frac{1}{e^2}\big(-e\cos(\theta+\beta)\left(u_1\sin\theta - V_t\sin\theta_t\right) + e\sin(\theta+\beta)\left(u_1\cos\theta - V_t\cos\theta_t\right)\big),$$

where from this, after some algebraic manipulation, it can be concluded (15).

□

Prepared using rncauth.cls
DOI: 10.1002/rnc

Analysis of the closed loop system in phase 2 with the control law (9)

The analysis is organized similar to what was done in the proof of Theorem 2. First, it will be shown that β is ultimately bounded with ultimate bound less than $\frac{\pi}{2}$ by appropriate choice of the gains. Using this fact, we then show the convergence of e.
Consider the dynamics of β (see (15)), which in closed-loop with the control law (9) satisfies

$$\dot{\beta} = \frac{k_3^a \tanh(k_3^b\, r)}{e} \sin\beta + k_4^a \tanh\left(k_4^b\,(\theta - \bar{\theta})\right) - \frac{V_t}{e}\sin(\beta + \theta - \theta_t), \tag{31}$$

and the positive definite function $V_1(\beta) \coloneqq \frac{1}{2}\beta^2$. Computing its time derivative along the trajectories of (31) and using the fact that $\theta - \bar{\theta} = -(\beta - \tilde{\bar{\theta}})$, one obtains

$$\dot{V}_1 \;=\; \beta\left[\frac{k_3^a \tanh(k_3^b\, r)}{e}\sin\beta - k_4^a \tanh(k_4^b\,(\beta - \tilde{\bar{\theta}})) - \frac{V_t}{e}\sin(\beta + \theta - \theta_t)\right].$$

Using the fact that $\sup_{0\le t\le t_f} |\tilde{\bar{\theta}}| \le \epsilon$ and applying the following trigonometric equality,

$$\tanh(z_1 - z_2) = (\tanh z_1 - \tanh z_2)/(1 - \tanh z_1 \tanh z_2)$$

we can conclude that for $|z_2| \le \epsilon$

$$-z_1 \tanh(z_1 - z_2) \le -a_1 z_1 \tanh(z_1) + a_2|z_1|$$

where $a_1 = \frac{1}{1+\tanh\epsilon}$, and $a_2 = \frac{\tanh\epsilon}{1-\tanh\epsilon}$. Thus, it follows that there exist constants $\alpha \in]0,1[$ and $\gamma \in]0,1[$ such that

$$\dot{V}_1 \le -k_4^a \frac{1}{1+\tanh(k_4^b\epsilon)}(1-\alpha)\beta\tanh(k_4^b\beta), \quad \forall \tanh|k_4^b\beta| > \gamma$$

and from this it can be concluded that β will be ultimated bounded with ultimate bound $\beta_a < \frac{\pi}{2}$ by suitable choice of the gains.

Now, the convergence of e will be examined. From (14), with u_1 as in (9), and using (27) the dynamics of e satisfies

$$\dot{e} = -k_3^a\ \tanh(k_3^b(e+f))\cos\beta + V_t\cos(\beta + \theta - \theta_t).$$

Using $V_2(e) \coloneqq \frac{1}{2}e^2$, we obtain

$$\begin{aligned}\dot{V}_2 \;&\le\; -k_3^a \frac{1}{1+\tanh(k_3^b R)} e\tanh(k_3^b e)\cos\beta + |e|\left(\frac{\tanh(k_3^b R)}{1-\tanh(k_3^b R)}\cos\beta + V_t\right)\\ &\le\; -k_3^a \frac{1}{1+\tanh(k_3^b R)} e(1-\alpha)\tanh(k_3^b e)\cos\beta, \quad \forall \tanh|k_3^b e| > \gamma\end{aligned}$$

Prepared using rncauth.cls
DOI: 10.1002/rnc

for some constants $0 < \alpha, \gamma < 1$. Thus, for any finite time $t \geq 0$, $e(t)$ is bounded (with no finite escape) and moreover, after a finite time t_1 with $|\beta(t_1)| < \frac{\pi}{2}$, $e(t)$ will converge to a neighborhood around zero.

REFERENCES

1. D'Andrea-Novel B, Campion G, Bastin G. Control of nonholonomic wheeled mobile robots by state feedback linearization. *International Journal of Robotics Research* Dec 1995; **14**(6):543–559.
2. Dixon W, Dawson D, Zergeroglu E, Behal A. *Nonlinear Control of Wheeled Mobile Robots*. Springer-Verlag: London, 2001.
3. Lawton JRT, Beard RW, Young BJ. A decentralized approach to formation maneuvers. *IEEE Trans. Robot. Automat.* Dec 2003; **19**(6):933–941.
4. Hauser J, Hindman R. Aggressive flight maneuvers. *Proc. of the 36th Conf. on Decision and Contr.*, San Diego, CA, USA, 1997; 4186–4191.
5. Kaminer I, Pascoal A, Hallberg E, Silvestre C. Trajectory tracking controllers for autonomous vehicles: An integrated approach to guidance and control. *J. of Guidance, Control, and Dynamics* 1998; **21**(1):29–38.
6. Al-Hiddabi S, McClamroch N. Tracking and maneuver regulation control for nonlinear nonminimum phase systems: application to flight control. *IEEE Trans. on Contr. Systems Tech.* 2002; **10**(6):780–792.
7. Godhavn JM. Nonlinear tracking of underactuated surface vessels. *Proc. of the 35th Conf. on Decision and Contr.*, Kobe, Japan, 1996; 975–980.
8. Encarnação P, Pascoal AM. Combined trajectory tracking and path following: an application to the coordinated control of autonomous marine craft. *Proceedings of the* 40^{th} *IEEE Conference on Decision and Control (CDC'01)*, vol. 1, Orlando, FL, USA, 2001; 964–969.
9. Behal A, Dawson D, Dixon W, Fang Y. Tracking and regulation control of an underactuated surface vessel with nonintegrable dynamics. *IEEE Trans. on Automat. Contr.* march 2002; **47**(3):495–500.
10. Do KD, Jiang ZP, Pan J. Underactuated ship global tracking under relaxed conditions. *IEEE Trans. on Automat. Contr.* Sep 2002; **47**(9):1529–1536.
11. Aguiar AP, Hespanha JP. Position tracking of underactuated vehicles. *Proc. of the 2003 Amer. Contr. Conf.*, Denver, CO, USA, 2003.
12. Pettersen KY, Nijmeijer H. Tracking control of an underactuated ship. *IEEE Trans. on Contr. Systems Tech.* 2003; **11**(1):52–61.
13. Aguiar AP, Hespanha JP. Trajectory-tracking and path-following of underactuated autonomous vehicles with parametric modeling uncertainty. *IEEE Transactions on Automatic Control* Aug 2007; **52**(8):1362–1379.
14. Arora A, Dutta P, S Bapat ea. A line in the sand: a wireless sensor network for target detection, classification, and tracking. *Computer Networks (Elsevier)* Dec 2004; **46**(5):605–634.
15. Crepaldi R, Casari P, Zanella A, Zorzi M. Testbed implementation and refinement of a range-based localization algorithm for wireless sensor networks. *Mobility06: Proceedings of the 3rd international conference on Mobile technology, applications & systems*, vol. 1, Bangkok, Thailand, 2006; 61.
16. Dil B, Dulman S, Havinga P. Range-based localization in mobile sensor networks. *Wireless Sensor Networks*, vol. 3868/2006, Romer K, Karl H, Mattern F (eds.). Springer-Verlag: Berlin Heidelberg, 2006; 164–179.
17. Gadre A, Stilwell D. Toward underwater navigation based on range measurements from a single location. *Proceedings of IEEE International Conference on Robotics and Automation (ICRA'04)*, vol. 5, New Orleans, LA, USA, 2004; 4472–4477.
18. Matveev AS, Teimoori H, Savkin AV. The problem of target tracking based on range-only measurements for car-like robots. *Proc. 49th IEEE Conference on Decision and Control*, Shanghai, China, 2009; 8537–8542.
19. Teimoori H, Savkin AV. Equiangular navigation and guidance of a wheeled mobile robot based on range-only measurements. *Robotics and Autonomous Systems* Feb 2010; **58**(2):203–215.

DOI: 10.1002/rnc

20. Zhang C, Arnold D, Ghods N, Siranosian A, Krstic M. Source seeking with non-holonomic unicycle without position measurement and with tuning of forward velocity. *Systems and Control Letters* march 2007; **56**(3):245–252.
21. Cochran J, Krstic M. Nonholonomic source seeking with tuning of angular velocity. *IEEE Trans. Automat. Control* Apr 2009; **54**(4):717–731.
22. Ghods N, Krstic M. Speed regulation in steering-based source seeking. *Automatica* Feb 2010; **46**(2):452–459.
23. Liberzon D. *Switching in Systems and Control*. Birkhauser: Boston, 2003.
24. Hespanha J, Morse A. Stability of switched systems with average dwell-time. *Proc. 38th IEEE Conference on Decision and Control*, Phoenix, AZ, 1999; 2655–2660.
25. Abramowitz M, Stegun I. *Handbook of Mathematical Functions With Formulas, Graphs, and Mathematical Tables.* Dover: New York, 1964.
26. Nesic D, Teel AR. Input-to-state stability for nonlinear time-varying systems via averaging. *Mathematics of Control, Signals, and Systems (MCSS)* 2001; **14**(3):257–280.

DOI: 10.1002/rnc